Optimization of THz quantum cascade lasers with an active module based on two-quantum wells for high-temperature operation

Optimization of THz quantum cascade lasers with an active module based on two-quantum wells for high-temperature operation

R A Khabibullin[1], D S Ponomarev[1], D V Ushakov[2] and A A Afonenko[2]

[1] V.G. Mokerov Institute of Ultra High Frequency Semiconductor Electronics, Russian Academy of Sciences, Moscow 117105, Russia
[2] Belarusian State University, Minsk 220030, Belarus

khabibullin@isvch.ru

Abstract. Over the past two decades, the operation temperature of terahertz quantum cascade lasers (THz QCLs) has continuously increased from cryogenic level to the current record value of 250 K (about -23ºC) [1]. Here we review the state-of-the-art and future prospects of high-temperature THz QCL designs with two-quantum wells in active module based on conventional heterojunction GaAs/AlGaAs and alternative material system HgCdTe. We have analyzed the temperature dependence of the peak gain and predicted the maximum operation temperatures of the given designs.

1. Introduction

Nowadays, there are many approaches to the generation of electromagnetic waves in the terahertz (THz) range, including down-conversion of optical femtosecond pulses [2], photomixing of two laser beams [3] and resonant-tunneling diodes [4,5]. Quantum cascade laser (QCL) is one of the spectrally brightest solid-state source of THz waves with a potentially wide range of practical applications in high-resolution spectroscopy [6,7] and imaging systems [8]. The main barrier to the use of THz QCL “outside the laboratory” is their low operating temperatures [9,10]. The limiting factors for increasing the operation temperatures of THz QCLs are associated with strong optical phonon scattering, the presence of parasitic current channels and the formation of electric field domains as was shown in [11,12]. In addition, the MBE growth of multilayered semiconductor structures for high-temperature THz QCL requires improvement [13,14]. Recently, the mode loss spectra for THz QCLs with double metal waveguide (DMW) were demonstrated in [15]. It was shown the high level of propagation loss of THz radiation in DMW, which exceeds 30 cm^{-1} for room temperature. Thus, to improve the high-temperature performance of THz QCLs it is needed to develop new concepts of active region designs and to reduce losses in DMW.

2. Optimization of the 2-well GaAs/AlGaAs active module

To calculate the THz QCL characteristics we have used the balance equation method with "tight-binding" wave-function basis. This basis has been obtained as superposition of eigenstates of the Schrödinger equation for the entire active region of a THz QCL by minimization of the spatial extension of wave functions of tunnel-coupled states. The localized ("tight-binding") basis is more

stable for dephasing impact, as degenerate basis states with $\Delta E \lesssim 3$ meV have a small overlap of wavefunctions and, correspondingly, a low self-scattering rate.

We have analyzed the 2-well designs based on GaAs/$Al_xGa_{1-x}As$ and optimized the height of potential barriers with different Al content (see Table 1). In Figure 1 we demonstrate the operation principle of the given designs and the current flow through the energy levels, indicated by red arrows. It is easy to notice that there are several current channels between electronic levels, including the 3-2 transition between the upper laser and lower laser levels, as well as the parasitic transitions 3-1. In Figure 2, we compare the temperature dependence of the peak gain at 3.9 THz and show the ability to operate above 200 K for designs with Al content x>0.2. For comparison, we demonstrate the calculated "gain vs temperature" dependence for 3-well design proposed in [16] with maximum operation temperature T_{max} = 210,5 K.

Table 1. Parameters of optimized 2-well designs of THz QCL based on GaAs/$Al_xGa_{1-x}As$.

	x	Barrier height U_0, (meV)	Layer sequence in period: **potential barrier**/quantum well, (nm)
Bosco design [16]	0.25	212.5	**1.98**/16.37/**3.39**/7.91
Design A	0.20	178.5	**2.3**/16.4/**4.2**/7.3
Design B	0.25	212.5	**2.0**/17.2/**3.4**/7.9
Design C	0.30	244.5	**1.7**/17.0/**3.1**/7.9

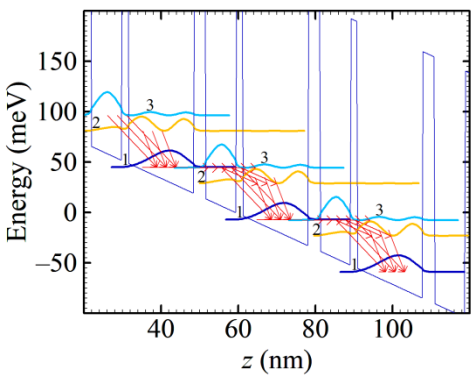

Figure 1. Conduction band diagram and squared modules of wavefunctions for GaAs/$Al_{0.3}Ga_{0.7}As$ design.

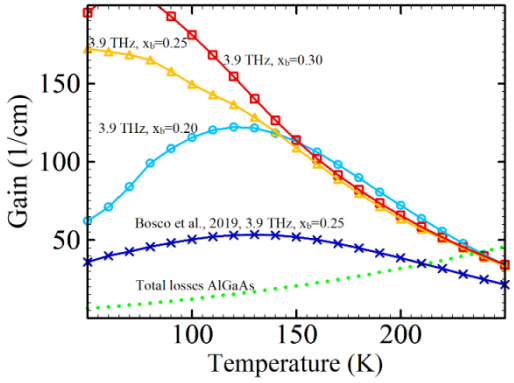

Figure 2. The temperature dependencies of peak gain are shown for GaAs/AlGaAs design with various Al content in barriers.

Optimization of designs with maximum gain at high temperatures (210–240 K) was obtained by scanning the active module thickness in the range from 24 to 36 nm. In this case, the thicknesses of the $Al_xGa_{1-x}As$ barrier layers varied in the range 1.4–4 nm, and GaAs quantum wells in the range 6.3–20 nm with a step equal to half the GaAs constant lattice. The parameters of the optimized active modules for various compositions of the barrier layers (Al contents) are presented in Table 1. In the layer sequence of active module, the GaAs quantum wells are shown in bold. The central part of the wide GaAs quantum well is Si-doped with a layer concentration of 4.5 10^{10} cm^{-2} as in [16].

The main factors affecting the gain in QCLs are: the electron effective mass m_c, the population inversion N_{32} of laser levels and matrix elements of dipole transitions Z_{32}. Thus, the gain of QCL active module can be represented as $G \sim m_c^{-3/2} N_{32} Z_{32}^2$. It means that the effective QCL amplification requires a low electron effective mass and a large population inversion and dipole matrix elements of

the transitions. The temperature dependences of these values for the optimized active modules in comparison with the Bosco design [16] are shown in Figure 3. It should be noted that the electron effective mass increases in designs with higher potential barriers (with higher Al content in $Al_xGa_{1-x}As$) due to the non-parabolicity effect as shown in Figure 3a. On the other hand, the m_c decreases at elevated temperatures for all designs. In the optimized designs B and C (Figure 3b), the population inverted is higher at temperatures above 200 K. As can be seen from Figure 3c, the matrix elements of dipole transitions of the given designs increase with an increase in temperature from 50 to 250 K: from 4.9 to 5.2 (Bosco 2019), from 4.7 to 5.0 (design A), from 4.4 to 4.7 (design B), and from 4.7 to 5.0 nm (design C). Thus, the combination of all 3 factors for all optimized designs A (x_b = 0.20), B (x_b = 0.25), and C (x_b = 0.30) gives the same predicted maximum operating temperature of 238 K.

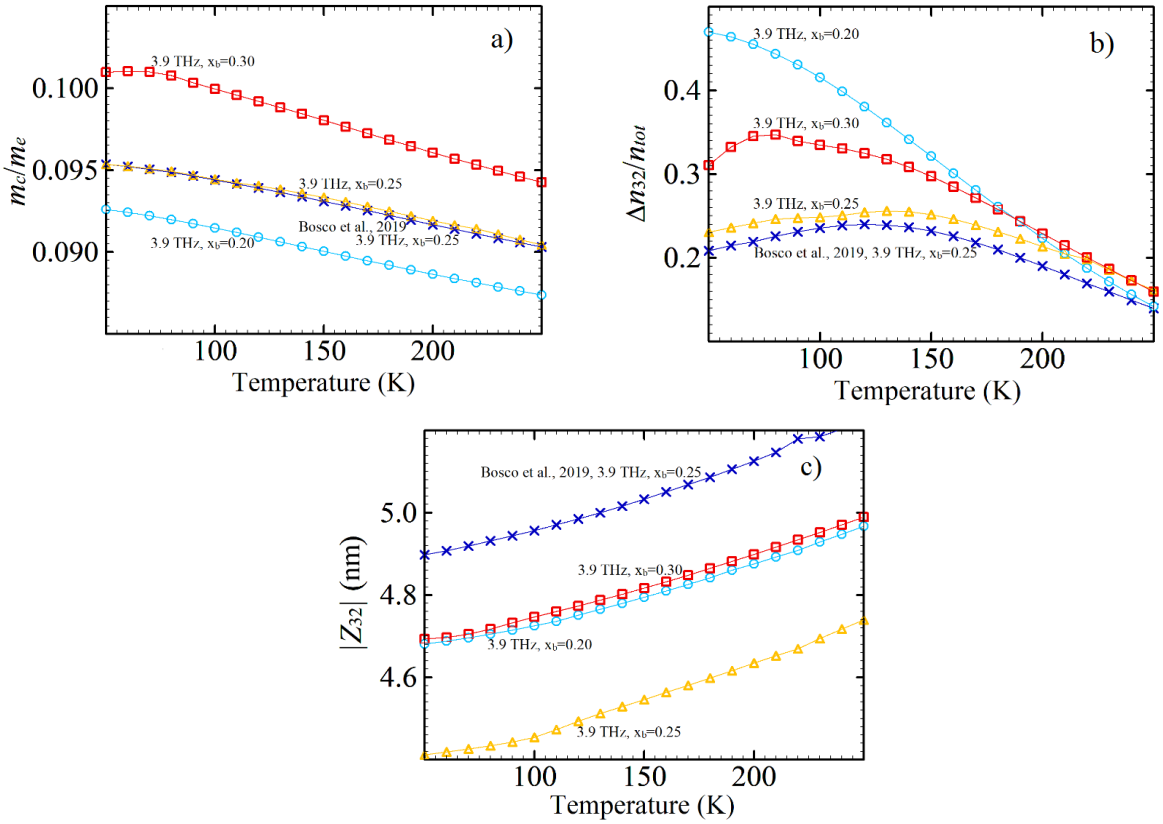

Figure 3. The temperature dependencies of a) electron effective mass m_c; b) population inversion Δn_{32} and c) matrix element of dipole transitions Z_{32} for optimized designs A (x_b = 0.20), B (x_b = 0.25), and C (x_b = 0.30).

3. Optimization of the 2-well HgCdTe active module

We simulate THz QCLs on the basis of narrow-gap HgCdTe quantum wells and calculate its characteristics. The characteristics of a single period, including current through localized states, leakage currents to continuum states, gain spectra and losses, were found by solving a system of balanced equations. We have proposed the 3-well and 2-well HgCdTe designs with maximum operation temperatures of 170 K and 225 K, respectively (see Figure 4) [17].

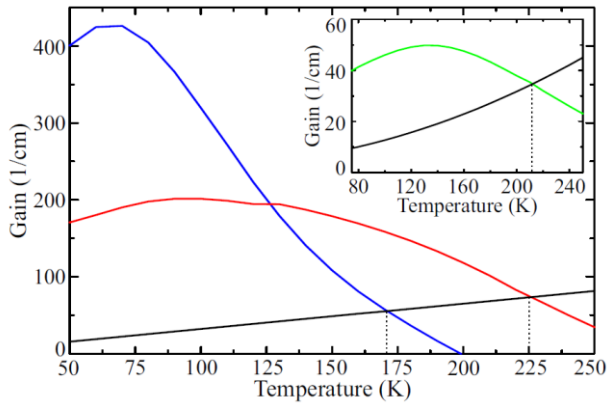

Figure 4. The temperature dependencies of peak gain are shown for the HgCdTe designs based on 3-well (blue line) and 2-well (red line), and for the GaAs/AlGaAs design based on 2-well of Bosco et al. [16] (green line in the inset). Cavity losses of a Cu-Cu waveguide is indicated by the black curves.

Acknowledgments
This work was supported by the Russian Science Foundation Grant No. 21-72-30020.

References

[1] Khalatpour A, Paulsen A K, Deimert C, Wasilewski Z R and Hu Q 2020 *Nat. Photonics* **15** 16
[2] Ilyakov I E, Shishkin B V, Malevich V L, Ponomarev D S, Galiev R R, Pavlov A Yu, Yachmenev A E, Kovalev S P, Chen M, Akhmedzhanov R A and Khabibullin R A 2021 *Opt. Lett.* **46** 3360
[3] Khabibullin R A, Morozov O G, Sakhabutdinov A Z and Nureev I I 2017 *Systems of Signal Synchronization, Generating and Processing in Telecommunications (SINKHROINFO)* 17080288
[4] Rasulova G K, Pentin I V, Vakhtomin Yu B, Smirnov K V, Khabibullin R A, Klimov E A, Klochkov A N and Goltsman G N 2020 *J. Appl. Phys.* **128** 224303
[5] Sobolev A S, Zaitsev-Zotov S V, Maytama M V, Klimov E A, Pavlov A Y, Ponomarev D S and Khabibullin R A 2021 *Opt. Eng.* **60** 082018
[6] Hubers H-W, Richter H and Wienold M 2019 *J. Appl. Phys.* **125** 151401
[7] Volkov O, Pavlovskiy V, Gundareva I, Khabibullin R and Divin Y 2021 *IEEE Trans. Terahertz Sci. Technol.* **11** 330
[8] Sterczewski L A, Westberg J, Yang Y, Burghoff D, Reno J, Hu Q and Wysocki G 2019 *Optica* **6** 766
[9] Khabibullin R A *et al* 2018 *Semiconductors* **52** 1380
[10] Volkov O Yu, Dyuzhikov I N, Logunov M V, Nikitov S A, Pavlovskii V V, Shchavruk N V, Pavlov A Yu and Khabibullin R A 2018 *J. Commun. Technol. Electron.* **63** 1042
[11] Khabibullin R A, Shchavruk N V, Ponomarev D S, Ushakov D V, Afonenko A A, Maremyanin K V, Volkov O Yu, Pavlopskiy V V and Dubinov A A 2019 *Opto-Electronics Review* **27** 329.
[12] Ushakov D V, Afonenko A A, Dubinov A A, Gavrilenko V I, Volkov O Yu, Shchavruk N V, Ponomarev D S and Khabibullin R A 2019 *Quantum Electronics* **49** 913
[13] Cirlin G E, Reznik R R, Zhukov A E, Khabibullin R A, Maremyanin K V, Gavrilenko V I and Morozov S V 2020 *Semiconductors* **54** 1092
[14] Reznik R R, Kryzhanovskaya N V, Zubov F I, Zhukov A E, Khabibullin R A, Morozov S V and Cirlin G E 2017 *J. Phys.: Conf. Ser.* **917** 052012
[15] Ushakov D V, Afonenko A A, Dubinov A A, Gavrilenko V I, Vasil'evskii I S, Shchavruk N V, Ponomarev D S and Khabibullin R A 2018 *Quantum Electronics* **48** 1005
[16] Bosco L, Franckie M, Scalari G, Beck M, Wacker A and Faist J 2019 *Appl. Phys. Lett.* **115** 010601
[17] Ushakov D, Afonenko A, Khabibullin R, Ponomarev D, Aleshkin V, Morozov S and Dubinov A 2020 *Opt. Express* **28** 25371